of 25μm through the whole thickness of the specimens.

Effects of Cu content and process conditions on mechanical properties in multi-layered Al-Zn-Mg alloy sheets

Katsushi Matsumoto[1], Masahiro Yamaguchi[1,*1] and Hiroshi Okuda[2]

1Materials Research Laboratory, Kobe Steel, Ltd., Kobe 651-2271, Japan
2Department of Materials Science and Engineering, Kyoto University, Kyoto 606-8501, Japan
**1Present address: Materials Solution Center, Technical Division, Kobelco Research Institute, Inc., 2-3-1, Arai-cho Shin-hama, Takasago 676-8670, Japan*

The age hardening behavior and nanostructure of the multi-layered Al-Zn-Mg alloy sheets with compositional gradient were investigated by tensile test, hardness test, electron probe microanalysis and scanning small angle X-ray scattering by micro beam, focusing on the effect of Cu addition. Cu added alloy improves the proof stress after natural and artificial aging by the distinctive hardness distribution through thickness direction. These characteristic hardness distributions are attributed to the formation of nano-sized precipitates during natural and artificial aging.

Keywords: *Al-Zn-Mg alloy, multi-layered sheet, small angle X-ray scattering, age hardening*

1. Introduction

Aluminum alloys have been used as structural applications in the automotive industry to reduce the vehicle body weight. One of the technical issues to meet these demands is the improvement of the multiple properties such as strength, ductility, press formability, corrosion resistance and weldability, which are essentially in a trade-off relationship with each other. In order to break through these limitations, multi-layered Al-Zn or Al-Zn-Mg alloy clad sheets with compositional gradient were proposed and investigated[1-3].

In the present study, age hardening behavior and nanostructure of the multi-layered Al-Zn-Mg alloy sheets with compositional gradient were investigated by tensile test, hardness test, electron probe microanalysis (EPMA) and scanning small angle X-ray scattering (SAXS) by micro beam, focusing on the effect of Cu addition.

2. Experimental Procedure

Five-layered aluminum alloy clad sheets with Al-Mg and Al-Zn alloys were studied. Figure 1 shows the detailed configurations of these specimens. These hot strips were stacked and bonded by rolling at 573K. Subsequent cold rolling to the final thickness of 1mm was performed. Heat treatment at 743K was conducted for the specimens to cause interdiffusion of the constituent elements across these layers and solid solution of them. After these heat treatments, these specimens were quenched into water and naturally aged at room temperature for 1.2Ms (T4), which was followed by artificial aging at 398K for up to 345.6ks. Concentration of the profile measurement through thickness was performed by EPMA. Mechanical properties were evaluated by tensile test. Hardness distribution was examined by micro-Vickers hardness test. Scanning SAXS by microbeam was performed to characterize the nanoscale precipitates in the multi-layered sheets at BL40XU of SPring-8. The X-ray, which has incident energy of 15keV, is shaped by a pinhole with a diameter of 5μm. The intensity distributions of SAXS were measured at intervals

From the detected two-dimensional SAXS spectra, the distribution of the integrated intensity, Q and the gyration radius, R_g was determined[4,5].

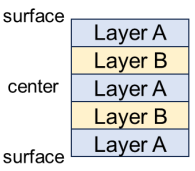

0Cu Layer A: Al-5.5Mg-0.06Zr-0.03Si-0.05Fe
Layer B: Al-9.1Zn-0.08Zr-0.04Si-0.06Fe

1Cu Layer A: Al-5.5Mg-0.06Zr-0.03Si-0.05Fe
Layer B: Al-9.8Zn-1.0Cu-0.09Zr-0.04Si-0.06Fe
(at%)

Fig.1 Configuration of the specimens and chemical compositions of the layers

3. Results and Discussion

Figure 2 shows the concentration distribution of the specimens after the annealing at 743K for 54ks. The constituent elements diffuse from the original layers, forming compositional gradient through thickness. Mg has its concentration peak at the first layer from the surface, whereas Zn and Cu at the second layer. As for the Cu added specimen 1Cu, the variation of Cu content through thickness varies from 0.08 to 0.79 at%, which is much smaller than those of other elements.

Figure 3 shows the hardness distributions, radius of gyration and integrated intensity through the thickness direction of the specimens 0Cu and 1Cu, and the proof stress in T4 condition. The hardness distribution (Fig.3(a)) corresponds to the profile of Zn element. The hardness of the specimen 1Cu is higher than that of the specimen 0Cu, in analogy with the proof stress. The 2D SAXS patterns, which indicate the presence of nano-sized precipitates, show isotropic scattering morphology, denoting the formation of spherical Zn-Mg clusters or G.P. zones. The radius of gyration for the precipitates inside the specimen

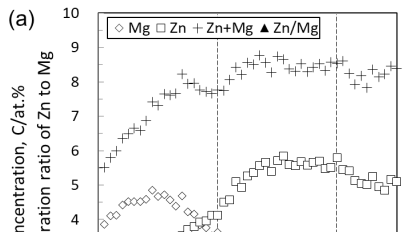

Fig.2 Concentration distributions of Mg, Zn, Cu, Zn+Mg and Zn/Mg through the thickness direction of (a) specimen 0Cu, (b) specimen 1Cu, after annealing at 743K for 54ks and subsequent natural aging for 1.2Ms.

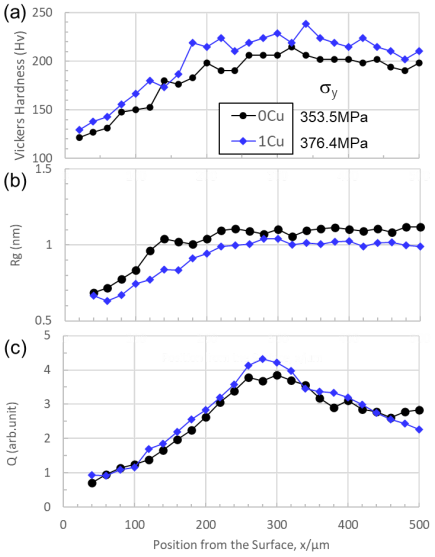

Fig.3 Distributions of (a) Vickers hardness, (b) radius of gyration (c) integrated intensity through the thickness of specimen 0Cu and 1Cu after annealing at 743K for 54ks and subsequent natural aging for 1.2Ms (T4). Proof stress is also indicated in (a).

(Fig.3(b)) is about 1nm, which is larger than that for the precipitates on the surface layer. The addition of Cu reduces the size of these precipitates. The distribution of the integrated intensity through the thickness direction (Fig.3(c)) corresponds to that of hardness. Moreover, the integrated intensity of the specimen 1Cu is larger than that of the specimen 0Cu. These results suggest that the addition of Cu accelerate the formation of finer precipitates in T4 condition.

Figure 4 shows the hardness distribution, radius of gyration and integrated intensity through the thickness direction of the specimens 0Cu, and the proof stress after artificial aging at 393K. The proof stress increases monotonically as artificial aging progresses, whereas the hardness distribution shows the distinctive changes; hardness in the range of 100μm from the surface decreases after artificial aging for 1.9ks (Fig.4(a)). Corresponding rapid increase in the radius of gyration (Fig.4(b)) and decrease in the integrated intensity (Fig.4(c)) suggest reversion of the clusters of G.P. zones on the surface layer at the early stage of artificial aging.

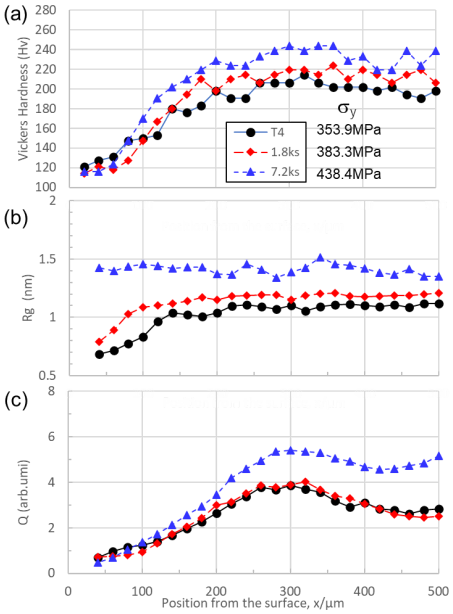

Fig.4 Distributions of (a) Vickers hardness, (b) radius of gyration, (c) integrated intensity through the thickness of specimen 0Cu after artificial aging at 393K. Proof stress is also indicated in (a).

Figure 5 shows the hardness distribution, radius of gyration and integrated intensity through the thickness of the specimens 1Cu, and the proof stress after artificial aging at 393K. The specimen 1Cu increase in hardness rapidly in almost all regions after artificial aging for 1.9ks (Fig.5(a)), resulting in the higher hardness distribution after artificial aging for 7.2ks than the specimen 0Cu. The integrated intensity for the specimen 1Cu is higher than that for the specimen 0Cu in any artificial aging conditions (Fig.5(c)). The 2D SAXS patterns for the specimen 1Cu after artificial aging for 7.2ks shows the more remarkable anisotropic scattering morphology, which indicates the formation of plate-like precipitates. These results suggest that Cu addition accelerate the transition of clusters or G.P. zones to metastable phases without reversion during the artificial aging, contributing to the increase in hardness.

In the phase decomposition process, the time change of the size of the precipitate during aging is expressed by the following equation; $R=R_0*t^n$, where R is the radius of the precipitates, t is time, n is the exponential coefficient[6]. Figure 6 shows the grain growth exponent of the precipitates for specimen 0Cu and 1Cu during artificial

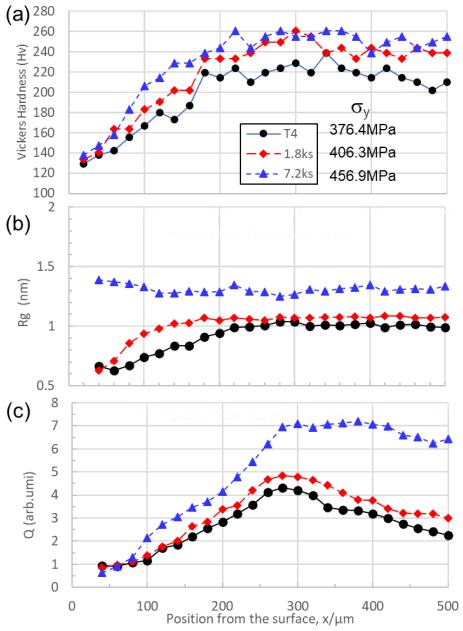

Figure 5 Distributions of (a) Vickers hardness, (b) radius of gyration, (c) integrated intensity through the thickness of specimen 1Cu after artificial aging at 393K Proof stress is also indicated in (a).

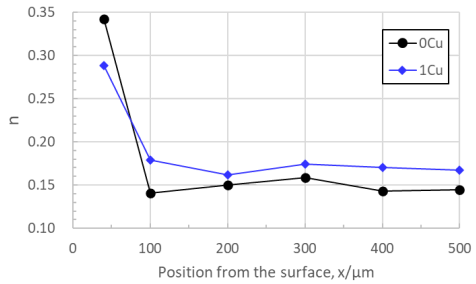

Figure 6 Grain growth exponent of the precipitates for specimen 0Cu, 1Cu during artificial aging at 393K.

aging at 393K. In the surface layer, it is interesting that the coefficient *n* is about 0.3, which is close to 1/3 in Ostwald ripening[7]. In the inner layers, on the other hand, the coefficient *n* of the specimen 1Cu is larger than that of the specimen 0Cu, suggesting that Cu addition promotes the growth of precipitates during artificial aging. This coefficient *n*, which is in the range of about 0.14 to 0.18, is close to 1/9 [8] reported previously. The coefficient *n* also tends to increase where the Zn concentration is high, which agrees with the previous report[6].

4. Summary

The age hardening behavior and nanostructure of the multi-layered Al-Zn-Mg alloy sheets with compositional gradient were investigated by tensile test, hardness test, EPMA and scanning micro-SAXS, focusing on the effect of Cu addition. Cu added alloy improves the proof stress after natural and artificial aging by the distinctive hardness distribution through thickness direction. These characteristic hardness distributions are attributed to the formation of nano-sized precipitates during natural and artificial aging.

Acknowledgement

This research is based on results obtained from a project, JPNP14014, commissioned by the New Energy and Industrial Technology Development Organization (NEDO). The synchrotron radiation experiments were performed at the BL40XU of SPring-8 with the approval of the Japan Synchrotron Radiation Research Institute (JASRI) (Proposal No. 2017A1597, 2017B1611).

References

1) K.Sato, K.Matsumoto and H.Okuda: Mater. Trans., 60 (2019) 254-262.
2) S.Lin, H.Okuda, Y.Higashino, K.Matsumoto and K.Sato: Mater, Trans., 61 (2020) 300-304.
3) S.Lin, H.Okuda, K.Matsumoto, M.Yamaguchi and K.Sato: Mater. Trans., 62 (2021) 603-609.
4) A.Guinier and G.Fournet: *Small-Angle Scattering of X-Rays*, (Wiley, NewYork, 1955).
5) H.Adachi, K.Osamura and H.Okuda: J. Japan Inst. Metals 63 (1999) 733-740.
6) T.Yamamoto, H.Adachi, H.Okuda, K.Osamura, K.Yokoe, J.Kusui and T.Yokote: J. Japan Inst. Light Metals, 48 (1998) 242-247.
7) T.Miyazaki: Materia, 53 (2014) 479-484.
8) C.E.Lyman and J.B.Vander Sande: Metal. Trans. A, 7A (1976) 1211-1216 .